Two-side laser processing method for producing high aspect ratio microholes

Nasrollahi, Vahid; Penchev, Pavel; Dimov, Stefan; Korner, Lars; Leach, Richard; Kim, Kyunghan

DOI:
10.1115/1.4037645
10.1115/1.4037645

Document Version
Peer reviewed version

Citation for published version (Harvard):
Nasrollahi, V, Penchev, P, Dimov, S, Korner, L, Leach, R & Kim, K 2017, 'Two-side laser processing method for producing high aspect ratio microholes', *Journal of Micro and Nano-Manufacturing*, vol. 5, no. 4, 041006 . https://doi.org/10.1115/1.4037645, https://doi.org/10.1115/1.4037645

Two-side Laser Processing Method for Producing High-Aspect Ratio Micro Holes

Vahid Nasrollahi[1]
Department of Mechanical Engineering, University of Birmingham, Edgbaston, Birmingham B15 2TT, UK
Vxn342@bham.ac.uk

Pavel Penchev
Department of Mechanical Engineering, University of Birmingham, Edgbaston, Birmingham B15 2TT, UK
p.penchev@bham.ac.uk

Stefan Dimov
Department of Mechanical Engineering, University of Birmingham, Edgbaston, Birmingham B15 2TT, UK
S.S.Dimov@bham.ac.uk

Lars Korner
Faculty of Engineering, University of Nottingham, University Park, Nottingham NG7 2RD, UK
Lars.Korner@nottingham.ac.uk

Richard Leach
Faculty of Engineering, University of Nottingham, University Park, Nottingham NG7 2RD, UK
Richard.Leach@nottingham.ac.uk

Kyunghan Kim
Korea Institute of Machinery & Materials, Daejeon, South Korea
khkim@kimm.re.kr

ABSTRACT

Laser micro processing is a very attractive option for a growing number of industrial applications due to its intrinsic characteristics, such as high flexibility and process control and also capabilities for non-contact processing of a wide range of materials. However, there are some constrains that limit the applications of this technology, i.e. taper angles on side walls, edge quality, geometrical accuracy and achievable aspect ratios of

[1] Corresponding author:
Vahid Nasrollahi, School of Engineering, University of Birmingham, Edgbaston, Birmingham B15 2TT, UK.
Vxn342@bham.ac.uk

produced structures. To address these process limitations a new method for two-side laser processing is proposed in this research. The method is described with a special focus on key enabling technologies for achieving high accuracy and repeatability in two-side laser drilling. The pilot implementation of the proposed processing configuration and technologies is discussed together with an in-process inspection procedure to verify the achievable positional and geometrical accuracy. It is demonstrated that alignment accuracy better than 10 µm is achievable using this pilot two-side laser processing platform. In addition, the morphology of holes with circular and square cross-sections produced with one-side laser drilling and the proposed method was compared in regards to achievable aspect ratios and holes' dimensional and geometrical accuracy and thus to make conclusions about its capabilities.

1-Introduction

There is an increasing demand for producing components incorporating micro-scale structures, especially in biomedical, optical, aerospace and automotive industries [1]. Key functional features of such components have sizes ranging from 1 to 100 µm, tolerances and surface roughness better than 5 µm and Ra 500 nm, respectively [2]. In response to this growing demand, manufacturing processes are developed to address issues related to the scalability of available technologies while achieving the required level of predictability, reproducibility, productivity and cost effectiveness in producing complex geometries in a variety of materials [3]. Both, conventional, e.g. micro milling or micro drilling, and non-conventional micromachining technologies have been used to produce such components. The non-conventional technologies used to produce micro-scale structures fall into three main categories [4]:

- Chemical and electrochemical, e.g. photochemical machining;
- Mechanical, e.g. ultrasonic and abrasive water jet machining;
- Thermal energy, e.g. electron beam, electric discharge and laser ablation.

Considering the material removal rate (MRR), the process reliability and capital investment required for cost-effective manufacture, together with components' technical requirements and batch sizes, a suitable process or processes can be selected among existing options. In some cases, especially for difficult-to-cut materials, hybrid machining solutions have been developed that combine the capabilities of two or more machining processes and thus to benefit from their complementarity in achieving acceptable manufacturing performance [2, 5, 6].

This research is focused on developing a new laser processing method that can be used for producing through structures, e.g. arrays of micro holes with high aspect ratio (depth to diameter ratio), that are required for a range of applications in the electronics industry, i.e. interconnecting vias and printed circuit boards, and also for producing interface probe cards for 3D wafer bumps [7-10]. The target holes' diameters and pitches in such applications are less than 60 μm, whereas the holes' aspect ratios are higher than 5 with taper angle less than 10°. These are very demanding requirements considering the accuracy, repeatability and throughput required for cost-effective processing and therefore there are limited numbers of micromachining processes that are capable of producing such hole arrays. In addition, it is important to state that there is a constant demand to reduce the holes' diameters down to 10 μm. In this context, one option is the use of photolithography to produce such through holes. However, photolithography requires multi-step processing in clean room environment that make this fabrication route capital intensive and thus potentially viable only for relatively high batch sizes [11]. Another manufacturing technology that could be employed is micro EDM drilling but this process has shortcomings too, i.e. high electrode wear and low MRR [12].

In the last decade, laser micro drilling has emerged as a viable alternative for producing such holes' arrays due to its intrinsic characteristics, such as high throughput,

capabilities for non-contact processing a wide range of materials and also for producing holes with diameters down to and even less than 10 μm. However, laser micro drilling has some limitations, too, such as tapered side walls, achievable geometrical accuracy and edge definition due to the heat affected zone (HAZ) and material spatters, and penetration depth constraints. Different research groups have investigated laser parameter domains, different process setups and drilling strategies to reduce and even eliminate these shortcomings. In particular, Adelmann and Hellmann [7] investigated the effects of different factors affecting the process and found that the accurate setting-up of the focal plane on the workpiece was the most influential one in producing holes with a very low taper and higher circularity in ceramic plates. Wang et al [13] tried to identify the best focus plane positioning to minimize the taper and HAZ. In particular, a drilling strategy was suggested to achieve as high as possible circularity of exit holes. Another aspect investigated by research groups was the use of assisted gases to facilitate the drilling process. For example, Khan et al [14, 15] studied the effects of different nozzle diameters and gases on achievable drilling rates. Hsu et al [16] employed an intermittent gas to minimize some side effects such as spatter and holes' taper, while Ho et al [17] compared the effects of swirling and straight gas on holes' depth. In addition, to process transparent materials such as sapphire a short pulse laser assisted wet etching was studied to attain high surface quality and efficiency for specific applications [18, 19]. Lott et al [20] investigated further to optimize the processing parameters such as repetition rate, pulse overlap and Z-axis translation speed and thus to drill 400μm holes in sapphire wafers while minimizing taper angle, drilling speed and cracks on the surface.

The use of different drilling strategies was also investigated by researcher, e.g. by using beam rotation apparatus for helical drilling [21], and thus to minimize/eliminate some side effects of the beams' Gaussian spatial profiles, i.e. micro cracks, circularity deviations and tapers. It is stressed that the selection of an appropriate drilling strategy is even more

important when high aspect ratio micro holes have to be produced as this has a major impact on the drilling condition. In particular, when percussion drilling is applied, with the increase of the pulse number the penetration rate decreases due to light scattering and blocking of the beam and deterioration of ablation and ejection conditions in general [11]. Even by applying high fluence, the hole depth achievable is limited because of multiple beam reflections from the holes' side walls and also due to re-depositioning of ejected/melted material [22]. Tokarev et al [23] reported that the absorption of the laser beam by the plasma plume and the effects of plasma stream doubled the wall heating because of radiation and convection, and also argued that this was the main reason for the different drilling conditions in deep and shallow holes. Therefore, it was proposed to model the plasma heating of side walls and thus to judge better about its effects on the drilling process.

In this paper, a new method for two-side processing is proposed to address some of the limitations associated with the laser micro drilling process. First, the distinguishing characteristics of the proposed method are described and the relevant research is reviewed. Then, the process design is discussed with a special focus on key enabling methods and technologies for achieving high accuracy and repeatability in two-side laser drilling. Next, a pilot implementation of the proposed method is described that is then used to validate the proposed two-side laser processing method. Finally, conclusions are made about the capabilities of the proposed method together with its enabling technologies based on the obtained experimental results.

2-Process characteristics and literature review

The concept for two-side laser drilling is simple. The operation requires first processing from one side until the saturation point is reached, i.e. when the penetration rate decreases substantially, and then after rotating the workpiece by 180^0 it continues from the opposite

side. The main advantages of this approach compared with one-side laser processing are [24, 25]:

1- The achievable aspect ratios can be doubled at least and thus to drill holes that cannot be produced due to their high aspect ratio.
2- The effect of taper angle that leads to considerable differences between the entry and exit holes' diameters can be eliminated.
3- The achievable processing efficiency is higher as drilling is performed only in its optimum processing window, i.e. the drilling process stops when the saturation point is reached.
4- Through holes with higher geometrical and dimensional accuracy can be produced as the number of pulses required is minimised and hence also the side effects associated with the laser drilling process.
5- The method is not limited to drilling only circular holes but can also be used for producing any structures, both through and blind, as high positional accuracy can be achieved in producing functional features from the two opposite sides of the workpiece [26].

Two-side holes' fabrication was reported only in two implementations and only one of them utilised laser processing. In particular, Wang et al [27] used such a method to produce 2 mm diameter holes employing electrochemical machining through a mask. The hole formation was studied step by step and then the method was applied to fabricate hole arrays with a lower taper angle. In another attempt, Goya et al [28] used the two-side method to drill a hole into a 62.5 μm glass optical fibre with a femtosecond laser and thus to fabricate a micro probe for spectroscopic measurements. It was reported that the micro holes produced from the two opposite sides connected successfully and thus it was possible to produce a through hole. The diameters of the holes were found to be approximately 10 and 18 μm at the waist

and at the fibre surface, respectively. The main focus of this research was the performance of a sensor produced with the proposed drilling method and not its capabilities in regards of achievable accuracy, repeatability and reproducibility that are essential in the production of dense holes' arrays with high efficiency.

To perform more than one side processing it is necessary to implement multi-axis laser processing machine configurations. Such multi-axis laser machining setups (machine tools) are available predominantly for macro-scale applications, i.e. for cutting, welding and drilling operations [29], but their use for multi-side precision machining has received less attention. In particular, some multi-axis laser micromachining setups were reported as pilot machine tool configurations to address specific application requirements. For example, a turning machine tool was reported for processing axisymmetric parts [30], while another research group proposed a laser milling process for producing freeform parts with functional features in the sub-millimetre range [31]. In other investigations 5 axis laser machining capabilities were demonstrated for fabricating complex parts, i.e. a micro globe and a micro windmill [32], while Jin et al [33] developed a mathematical model for compensating volumetric errors in multi-axis laser processing after singling out geometrical errors associated with each axis.

Laser processing systems commonly integrate scan heads that are usually combined with mechanical stages to realise complex multi-axis micromachining configurations. The scan heads allow high dynamic beam movements but with a relatively low accuracy limited to a relatively small working envelop (field of view) compared with those achievable with the CNC mechanical stages [34]. This is another important difference between laser-based machining systems and conventional CNC machine tools. Recognising these significant differences, solutions were reported to address the constraints associated with them in implementing multi-axis laser micromachining setups. In particular, Kim et al [35] reported a software solution to synchronize the movements of mechanical stages and beam deflectors of

a scan head, and thus to process bigger areas than the field of view, with acceptable accuracy and speed. At the same time, Penchev et al [36] reported generic software tools to minimize the negative dynamic effects of scan heads on achievable accuracy and also to benefit fully from available high frequency laser sources [37]. In addition, generic integration tools, i.e. a modular workpiece holding device, an automated work-piece setting up routine and an automated strategy for multi-axis processing employing rotary stages, were proposed for improving the system-level performance of laser micromachining systems [38].

3- Process design

3.1- Background and sources of errors

As it was stated above machining from two-sides is a relatively simple concept but its complexity increases when high accuracy, repeatability and reproducibility have to be achieved. In particular, the difficulties arise from the necessary high precision alignment of the holes/structures produced from two sides. This is due to geometrical errors in rotating the workpieces by 180^0 employing rotary stages. There are two main methods to execute such a drilling strategy: (i) quantifying various sources of errors and then compensating them; or (ii) implementing fully automated routines. In this research, the main focus is on designing and validating automated routines.

To design such routines it is essential to identify first the sources of errors in two-side drilling and then to plan a sequence of steps necessary to execute fully automated drilling operations while minimising the effects of these errors. Generally, the error sources in CNC machining operations can be grouped as follows [39]:

i. **Thermal errors**. They are negligible in laser micro processing (LMP) since the laser sources used are with a very low average power and they are usually kept away from the processing area. In addition, most of the movements are carried out with beam deflectors (scan heads) and not with mechanical axes.

ii. **Cutting-force induced errors**. There are no such errors in LMP as it is a non-contact method.

iii. **Geometric and kinematic errors associated with linear and rotary axes**. In particular, for each linear axis there are two straightness, one positioning, and three angular errors (pitch, yaw, roll) while for rotary axes there are two radial, one axial, two tilt and one angular positioning error. Also, there are five location errors associated with rotary axes and three squareness errors accompanying the linear axes [40].

Thus, only the last class of geometrical errors are critical in executing precise laser machining operations and therefore should be considered in designing two-side laser drilling operations. In addition, there are other compensation movements that are specifically required in executing two-side drilling routines, i.e. due to:

- *Incident beam is not normal to the workpiece:* It is shown in Figure 1a and b that angular displacements of the beam from the workpiece surface normal (it is assumed that the beam is parallel to the Z axis) in regards to A ($\Delta\alpha°$) or B ($\Delta\beta°$) axes (realised with two rotary stages) can be compensated by repositioning in the Y and X directions respectively. However, a through hole drilled from two sides will not be normal to the workpiece and therefore it is essential to minimise any angular displacements in both directions before executing drilling operations. For simplicity only the displacement between the A axis and the beam is discussed further in this section but the considerations apply to the B axis, too.

- *Incident beam is not perpendicular to A axis:* As it is shown in Figure 1c, although such angular displacement ($\Delta\psi°$) can be compensated by repositioning in the X direction, the holes drilled from two sides will not be coaxial and therefore this error has be minimised again to an acceptable deviation range.
- *Displacement of hole positions in respect to A axis:* Depending on the displacement of holes from the A axis, the workpiece needs to be repositioned twice in the Y direction and thus to align the holes drilled from the two opposite sides as shown in Figure 2a.
- *A axis not being parallel to X axis*: As it is shown in Figure 2b, this error can be compensated by measuring the angular displacement, $\Delta\gamma$, and then calculating the required compensation movements of the X and Y stages, based on the hole position.
- *Displacements between A axis and the centre plane of the workpiece in Z direction are higher than the laser beam depth of focus (see Figure 3):* Such a displacement can lead to an offset of the beam focal plane after rotating the workpiece by 180º. This can be compensated with repositioning movements in the Z direction and thus to adjust the focal distance.
- *Dynamic limitations of beam deflectors* should be considered by finding the optimum laser delays [36].
- *Beam displacements in machine coordination system (MCS)* caused by alignments and calibrations of the optical components or changing ambient conditions [41].
- *Deviations from the parallelism of mechanical and optical axes* in executing the operations.
- *Linear and rotational positioning errors:* These errors need to be considered especially for the movements in the X and Y directions and also for the A axis to minimise any undesirable radial and axial displacements as a result of the rotation by 180º.

There are some other general considerations, such as sample flatness, that have to be taken into account in designing the process. Most of the potential errors listed above are systematic and can be substantially reduced by quantifying them and then calculating the required linear and rotary adjustments of the workpiece. However, residual errors associated with the required measurements, and linear and rotary movements cannot be compensated. These errors are directly dependent on the measurement equipment and the linear/rotary stages used, and can be minimised by increasing their precision, so as to reduce their combined effects.

3.2- Design and requirements

To execute two-side laser drilling operations with required accuracy, repeatability and reproducibility it is necessary to design and implement a laser processing configurations for their automation, including the necessary calibration and setting up routines. Therefore, it is important to develop an automated method that minimises and even eliminates any pre-trials in achieving a higher precision without increasing the process uncertainty. The implementation of fully automated two-side laser drilling operations requires not only component technologies that are always necessary to realise laser processing operations but also those required to realise multi-axis processing, specialised workpiece handling and automated process setting up routines. In particular, the first group of component technologies includes those that are selected taking into account the workpiece material, required beam spot diameter and target structure dimensions and quality, i.e. laser sources, beam conditioning devices, scan heads and focusing lenses. The second group includes additional component technologies, both hardware and software tools, that are specially

configured and/or developed to address the specific requirements associated with the two-side laser drilling operations and thus to execute them with the necessary accuracy, repeatability and reproducibility. The requirements of component technologies that should be specially configured and/or developed for carrying out such drilling operations are discussed below.

3.2.1- Rotary mechanical stages

To carry out two-side laser processing, one rotational axis is required and therefore the machine configuration should integrate at least one rotary stage. The general requirements that such a stage should satisfy are:

- *The rotational axis should be perpendicular to the incident laser beam*. Assuming that the laser beam is parallel to the Z axis in the setup design, the rotary stage should realise A (rotation around X axis) or B (around Y axis) axes. Figure 1c depicts how an angular displacement of the incident beam from perpendicularity to the A axis can affect directly the concentricity and coaxiality of holes by $\Delta\psi°$. In this research, an A rotary stage was used however two-side drilling operations could be implemented with a B stage in the same way.
- *Pre-defined resolution and repeatability in realising rotations by 180°*. The angular deviations in executing such rotations can be compensated but only down to the stage resolution. Also, if such deviations are stochastic for a given processing strategy, they can directly affect not only the holes' coaxiality but also their positional accuracy. Thus, the rotary stage has to be selected taking into account the holes' positional and geometrical accuracy.
- *The rotary axis should be parallel to the X or Y axes.* Such angular displacements of $\Delta\gamma$, as shown in Figure 2b, can be compensated but require additional adjustment in X and Y directions, which could be avoided.

- *Minimised axial and radial errors.* Such errors can be compensated but only if they are systematic and therefore the achievable accuracy can be in the order of the rotary stage repeatability.

If the processing configuration integrates A and B rotary stages, drilling strategies can be designed to compensate any primary tilting of the workpiece in both directions (see Figure 1a and 1b). In addition, the integration of a C stage will allow in-process setting up and inspection routines to be automated.

3.2.2- Linear mechanical stages

The implementation of two-side laser processing requires a range of positional movements as discussed in Section 3.1. These movements introduce the following requirements in selecting the linear stages for executing automated laser drilling routines.

- *X and Y stages* have to be used in routines for detecting automatically the positions of reference marks/features, e.g. a reference through hole, before and after the rotation of the workpiece and also for correlating the beam coordination system (BCS) to the MCS. Hence, the accuracy and resolution of these stages directly affects the achievable accuracy.
- *X and Y stages* should ensure precise initial positioning of the workpiece and then the necessary linear adjustments after the rotation by 180^0. These X/Y movements are required to position the workpiece in the field of view of different sensors for process setting up and inspection. Therefore, the repeatability of the stages in executing these movements is essential for achieving the required positional accuracy of the holes.
- *The Z stage* should keep the workpiece within the laser beam depth of focus before and after the rotation by 180^0. Hence, the resolution and repeatability of the Z stage should be better than the Raleigh length of the focused laser beam.

- *The straightness and angular errors of the linear stages* can be compensated automatically but their repeatability is important for achieving the required positional accuracy of the holes.

3.2.3- Modular workpiece holding device

The implementation of the two-side laser drilling method requires the development of a specialised workholding device to ensure the beam access to both sides of workpieces and a reliable, and at the same time, flexible interface between the workpiece and the stack of the mechanical stages in the laser drilling setup. Therefore, the workholding system should have a modular design and should be easily adaptable to workpieces with different sizes and shapes. In addition, the overall size and mass should be minimised to lessen the negative dynamic effects in executing precision movements with a stack of mechanical linear and rotary stages, and cover the least possible surface area of the workpiece. In spite of fact that laser drilling is a non-contact process, the workpiece fixturing should be sufficiently reliable, especially during or after the rotation by 180^0, to eliminate any additional errors in the workpiece-workholding devise sub-system.

3.2.4- System level tools

Alignment/measurement probes. To correlate the workpiece coordinate systems (WCS) to MCS, non-contact measuring probes, e.g. a chromatic confocal probe, should be employed to detect reference marks/features with the required level of accuracy and precision and also to determine the position the workpiece surface along the laser beam propagation direction (the focal plane). The working area of the probe should be easily accessible with the use of mechanical stages to determine the X, Y and Z positions of workpiece reference features/surfaces. The accuracy and resolution of the probe should be selected 5 to 10 times higher than the target positional accuracy of the laser drilled holes. Other important

characteristics of the probe that determine its alignment/inspection capabilities are its working distance and the measurement range.

Fully automated process setting up routines. Process setting up routines should be developed for executing two-side laser drilling operations that employ the alignment/measurement probe to assess the errors from various sources discussed in Section 3.1 and then to compensate or minimise their impact on the process accuracy and repeatability. In particular, these routines should automate the following process setting up steps:

- Correlating the A axis to the BCS and thus to compensate radial displacement in the Y direction due to rotations with the A stage.
- Measuring the angular displacement between the X and A axes ($\Delta\gamma$);
- Measuring axial displacements of the A stage (ΔX_A) due to rotations around the A axis.
- Measuring angular displacement after executing a rotation by 180° with the A stage ($\Delta\theta$).
- Determining the focal planes of the laser beam on the workpiece, i.e. the initial setting up of the laser drilling process and then after the rotation by 180^0, to compensate any radial displacements in the Z direction.

An automated process setting up that includes the above set of routines is described in Section 3.3. In addition, to set the drilling process, the laser parameters have to be optimised to achieve the required quality and throughput. This should include determining the optimum pulse number after which the penetration rate decreases substantially (the saturation point) or the mid plane of the workpiece is reached and thus to know when to continue the drilling process from the opposite side. In particular, the maximum possible thickness of the workpiece that can be drilled by this method can be estimated to be up to twice the maximum depth of blind holes or the saturation point in one side drilling.

In-process inspection methods. To automate the drilling process fully it is recommended to develop in-process methods for monitoring the drilling process. This can be achieved by integrating in the process setup a 3D metrology sensor to carry out in-process inspections, i.e. dimensional and other measurements to judge about accuracy and general quality, but also to monitor the alignment accuracy of the holes/structures produced from two sides. Such a sensor should utilise the linear and rotary stages integrated in the laser processing setup to perform inspection and monitoring routines on both sides of the workpieces. Therefore, the sources of errors should be identified and thus to calculate the combined uncertainty associated with different measurement procedures. The ultimate objective should be to select a 3D metrology sensor in such a way that the combined uncertainty associated with the in-process measurement routines does not exceed a fifth of the required positional accuracy of the drilled holes.

3.3- Fully automated process setting procedure

The procedure employs reference through features, i.e. two through holes produced from one side, to minimise the effect of various error sources (see Section 3.1) by implementing the routines outlined in Section 3.2.4. Figure 4 depicts the overall concept of finding the centres of two reference holes, located at Points 5 and 6 respectively, on the first side of the workpiece. Then, the centres of the two holes, i.e. Points 7 and 8 in Figure 4, are found again after rotating the workpiece by 180^0 and thus to calculate the resultant axial displacement of ΔX_A. The radial displacements in the Y and Z directions, resulting from the rotation, are compensated by correlating the A axis to the BCS and some adjustments in the Z direction. With this reference data, it is possible to determine the centres of all holes that have to be drilled on the workpiece after the rotation. More than two through holes can be used as references to minimise the effects of any errors in their manufacture.

This process setting up procedure requires the execution of the following steps as depicted in Figure 4:

1. Positioning the workpiece under a non-contact probe, scanning its surface in the X_{MCS} and Y_{MCS} directions using the mechanical stages to find the initial angular displacements of the workpiece normal relative to Z_{MCS} and then compensating them by rotating the workpiece around the A_{MCS} and B_{MCS} axes.
2. Determining the focal plane and its respective Z_{MCS} value and thus to ensure that the first side of the workpiece (z_1) is within the laser beam depth of focus.
3. Laser drilling of two through holes with well-defined edges, e.g. 500 µm in diameter, that are positioned as far as possible from each other.
4. Positioning the probe beam inside the first hole (Point 0) by using X and Y mechanical stages.
5. Scanning the hole along the X_{MCS} direction to detect Points 1 and 2 and thus to find the X_{MCS} coordinate (X_5) of the reference hole centre (Point 5).
6. Scanning of the hole along the Y_{MCS} direction to detect Point 3 and 4 and thus find the Y_{MCS} coordinate (Y_5) of the reference hole centre (Point 5).
7. Positioning of the probe beam inside the second hole and repeating Steps 5 and 6 to find the X_{MCS} and Y_{MCS} coordinates (X_6 , Y_6) of its centre (Point 6).
8. Rotation of the workpiece by 180° around the A_{MCS} axis.
9. Scanning the workpiece surface in the Y_{MCS} direction to find the angular displacement ($\Delta\theta$) of the workpiece normal in regards to Z_{MCS}.
10. Repeating Step 2 for the second side of the workpiece to ensure again that the workpiece is within the laser beam depth of focus (z_2).
11. Repeating Steps 4 to 6 for the two reference holes on the second side and thus to find the X_{MCS} and Y_{MCS} coordinates of their centres, i.e. Points 7 and 8 (X_7 , Y_7 and X_8 , Y_8).

Based on the results, i.e. X_{MCS} and Y_{MCS} coordinates of Points 5 to 8, obtained with this process setting up procedure, the angular displacement between the A_{MCS} and X_{MCS} axes ($\Delta\gamma$), the axial error (ΔX_A), and the position of the A_{MCS} axis can be calculated by employing Eq. (1) and (2):

$$X_7 - X_5 = \Delta X_A + (Y_5 - Y_7) \cdot \tan(\Delta\gamma), \quad (1)$$

$$X_8 - X_6 = \Delta X_A + (Y_6 - Y_8) \cdot \tan(\Delta\gamma). \quad (2)$$

By solving Eq. (2), $tan(\Delta\gamma)$ and ΔX_A are calculated, i.e.:

$$\tan(\Delta\gamma) = \frac{X_7 - X_5 - X_8 + X_6}{Y_5 - Y_7 - Y_6 + Y_8}, \quad (3)$$

$$\Delta X_A = X_7 - X_5 - \frac{(Y_5 - Y_7)(X_7 - X_5 - X_8 + X_6)}{Y_5 - Y_7 - Y_6 + Y_8}. \quad (4)$$

The general formula for calculating the symmetry points (x, y) in relation to a line, $Y = a.X + b$, would be:

$$\left(\frac{x(1-a^2)+2a(y-b)}{a^2+1}, \frac{2(ax+b)-y(1-a^2)}{a^2+1}\right). \quad (5)$$

In this research, the symmetry line $Y = a.X + b$ is the A_{MCS} axis and $a = \tan(\Delta\gamma)$. Using Eq. (5) and the coordinates of Points 5 and 7, b_1 can be calculated as follows:

$$b_1 = \frac{Y_7(a^2+1)+Y_5(1-a^2)}{2} - a.X_5, \quad (6)$$

and then b_2 using Points 6 and 8:

$$b_2 = \frac{Y_8(a^2+1)+Y_6(1-a^2)}{2} - a.X_6. \quad (7)$$

Ideally b_1 and b_2 should be equal. However, because of the uncertainties in finding the coordinates of Points 5 to 8 there may be a difference between them. Therefore, to minimise this offset their average can be taken:

$$b = \frac{b_1+b_2}{2}. \quad (8)$$

Based on this process setting up procedure, it would be possible to execute a sequence of steps to produce an array of holes, i.e.:

- Producing the array of holes with coordinates (X, Y, z_1) on the first side by using a pre-defined number of pulses necessary to reach the saturation point or workpiece mid plane;
- Rotation by $180^0+\Delta\theta$ around the A_{MCS} axis to set the second side of the workpiece and thus to continue the drilling operation and also to compensate any rotational errors;
- Positioning the workpiece at z_2 along the Z_{MCS} axis to compensate any radial errors as a result of the rotation and any displacements between the centres of rotation and the workpiece (see Figure 3) and thus to set the focal plane of the workpiece on the second side within the laser beam depth of focus;
- By using the calculations of Eq. (3), (4) and (8), the X_{new} and Y_{new} coordinates of each hole on the workpiece's second side are determined as follows:

$$X_{new} = \frac{X\left(1-tan^2(\Delta\gamma)\right)+2.\tan(\Delta\gamma).(Y-b)}{tan^2(\Delta\gamma)+1} + \Delta X_A, \quad (9)$$

$$Y_{new} = \frac{2(\tan(\Delta\gamma).X+b)-Y\left(1-tan^2(\Delta\gamma)\right)}{tan^2(\Delta\gamma)+1}. \quad (10)$$

By applying Eq. (9) and (10), the axial rotational error (ΔX_A) and angular displacement between the X_{MCS} and A_{MCS} axes ($\Delta\gamma$) are compensated. Also, the position of the A_{MCS} axis in MCS is determined and thus the radial rotational error in the Y_{MCS} direction is also compensated.

3.4. In-process inspection methodology

It is necessary to implement in-process monitoring and inspection methods within the laser processing setup without moving the workpiece as outlined in Section 3.2.4. In particular, the workpiece can be positioned in the field of view of the 3D metrology sensor by employing the C, X, Y and Z mechanical stages of the laser processing setup and thus to carry out in-process inspection routines on both sides of the workpiece. As the 3D sensor is integrated in the laser processing setup, the alignment accuracy between pairs of holes on two opposite sides of the workpiece can be assessed by using as references through features, e.g. through holes, in the sensor coordination system (SCS). In this way, the combined uncertainty can be minimised as both the reference features and the through micro holes are within one field of view of the sensor. The in-process inspection procedure to assess the alignment accuracy of the proposed drilling method includes the following steps:

1) Laser drilling of a reference through feature from one-side, e.g. a 500 µm circular hole but through structures with other cross-sections can be used, too;
2) Percussion drilling a through micro hole employing the two-side drilling operation;
3) Positioning the reference and micro holes within the sensor field of view using the mechanical axes as shown in Figure 5a;
4) Finding the coordinates (X_9, Y_9 and X_{10}, Y_{10}) of the reference and micro holes' centres in the SCS, i.e. Points 9 and 10, respectively;
5) Rotating the sample by 180° with the rotary stage and repeating Steps 3 and 4 to find the coordinates (X_{11}, Y_{11} and X_{12}, Y_{12}) of the two holes on the second side in SCS, i.e. Points 11 and 12 in Figure 5b.
6) Calculating the displacement between the holes on the two sides as follows:

$$\Delta X_{s1} = X_{10} - X_9\,, \Delta Y_{s1} = Y_{10} - Y_9\,, \quad (11)$$

$$\Delta X_{s2} = X_{12} - X_{11}\,, \Delta Y_{s2} = Y_{12} - Y_{11}. \quad (12)$$

If the angular displacement between A_{MCS} and X_{SCS} is $\Delta\emptyset$, based on Eq. (5), the errors in X and Y directions are:

$$E_X = \Delta X_{s2} - \frac{\Delta X_{s1}\left(1-tan^2(\Delta\emptyset)\right)+2\tan(\Delta\emptyset).\Delta Y_{s1}}{tan^2(\Delta\emptyset)+1}, \quad (13)$$

$$E_Y = \Delta Y_{s2} - \frac{2\tan(\Delta\emptyset).\Delta X_{s1}-\Delta Y_{s1}\left(1-tan^2(\Delta\emptyset)\right)}{tan^2(\Delta\emptyset)+1}), \quad (14)$$

$$E = \sqrt{E_X^2 + E_Y^2}. \quad (15)$$

$\Delta\emptyset$ is an important factor affecting the precision of this in-process alignment assessment method. Therefore, the effects of such angular displacement should be minimised during the integration of the 3D metrology sensor into the laser processing setup. In addition, this displacement can be measured with the optical sensor and hence can be taken into account in Eq. (13) and (14). However, the uncertainty associated with this alignment measurement needs to be included in the uncertainty evaluation of the proposed two-side drilling method. Other limitations of this in-process inspection method is the finite sensor field of view but it is possible to extend it by stitching fields together employing software tools.

It should be stressed that an important advantage of this in-process inspection method is that the sources of errors discussed in Section 3.1 (those associated with the two-side drilling method) do not affect it, too.

3.5 In-process measurement uncertainty

To apply the proposed in-process measurement, uncertainties associated with this method should be determined. In particular, to determine to what extend it is possible to trust the alignment accuracy results when measuring holes produced using the two-side drilling method. Therefore, the expanded uncertainties associated with the proposed validation procedure have to be assessed. In this research this is carried out based on the GUM guide [42].

Essential part in determining the uncertainty of a measurement procedure is to identify the sources of errors that affect all its steps, especially to evaluate the uncertainties associated with them. In particular, the use of 3D metrology sensor to assess the alignment accuracy of the holes produced with the two-side drilling method involves a number of steps and the associated uncertainties with them have to be considered, i.e.:

U1. and U2. The uncertainty in measuring the micro holes' centres on two opposite sides of the workpiece.

U3. The uncertainty in measuring the reference through structure, e.g. the through hole used in this research, on the first side of the sample.

U4. The uncertainty in measuring the reference hole on the second side of the sample. It is calculated as U3, however since the reference hole is laser drilled from the first side, the edge definition and quality of its entrance and exit will defer. Hence, the uncertainties in determining the coordinates of their centres should be considered separately.

U5. The uncertainty associated with the use of a through hole to correlate SCSs on the two sides. Since the through holes are laser drilled, they will have a taper angle that can result in some variations of their centres on its entrance and exit sides. This can affect directly the

precision of the alignment procedure and thus increases its uncertainty. Therefore, it is necessary to assess it, too.

U6. Uncertainty of detecting the angular displacement between the A_{MCS} and X_{SCS} axes which should be transformed into a lateral uncertainty to calculate the expanded uncertainty.

All of the above uncertainties are evaluated as type A, i.e. they should be calculated by using statistical methods. In addition, one type B is considered, i.e.:

U7. The resolution of the C stage. If the C stage is used to position the workpiece in the sensor field of view, the uncertainty associated with this rotation should be considered. In particular, the resolution of the rotary stage affects $\Delta\emptyset$.

4. Experimental validation

4.1. Material

The automated two-side drilling operation can be used for any material that can be processed by a given laser source. In this research it is validated on silicon nitride (Si_3N_4) substrates. This material has a wide application in microelectronic and microelectromechanical systems because of its properties such as insulation capabilities and its resistance in high-energy manufacturing processes [43].

The thickness of the silicon nitride substrate used in this research was 250 μm and the surface roughness of the sample was measured with a focus variation microscope (Alicona G5), i.e. *Sa* of its two sides was 220 nm.

4.2. Equipment

The automated two-side drilling operation was validated on a laser micro processing platform that integrates the following key component technologies:

- 5 W Yb-doped sub-pico laser source with wavelength of 1030 nm, pulse duration of 310 fs, frequency up to 500 kHz and beam quality factor M^2 better than 1.3;
- A telecentric lens with 100 mm focal length exchangeable with a drilling/cutting head that integrates a 50 mm focusing lens as shown in Figure 6b;
- High precision X and Y mechanical stages with linear motors for positioning the workpiece with a resolution of 250 nm and repeatability of ±0.75 µm;
- Two rotary stages to position the workpiece around the X axis (A) and the Z axis (C) with resolution and repeatability of 3.15 µrad and ±19.4 µrad, respectively. The A axis is a key component for implementing the proposed two-sides drilling method;
- A chromatic confocal probe [44] for executing the automated process setting up procedure described in Section 3.3. The probe axial resolution is 130 nm with spot radius of 3.6 µm and measuring range of 4 mm (Figure 6a);
- An integrated focus variation probe, i.e. Alicona IF-Sensor R25, with a 10× objective lens that has: wield of view of 2 x 2 mm, a working distance of 15.5 mm, a vertical resolution of 100 nm and sampling distance of 1 µm (Figure 6c);
- A specially designed modular workholding device to provide a laser beam access to both sides of a workpiece as depicted in Figure 6. As it is shown in the Figure 7, the device includes an adapter and spacers and thus the laser processing setup can accommodate workpieces with different sizes and thicknesses.

4.3 Percussion drilling

As stated in Section 3.2.4 to setup the process it is necessary to determine the optimum pulse number after which the penetration rate decreases substantially. To do so, arrays of blind holes with a varying number of pulses was produced and their depth measured. The other laser parameter settings that affected the penetration depth were the pulse frequency and energy. They were selected based on the results reported by other researchers [45-48] and also the author's experience with the laser source used in this research. In particular, the following laser settings were selected, pulse frequency of 100 kHz and average power 0.68 W. The focal plane was kept at the substrate surface to drill arrays of blind holes.

The depth of the produced blind holes was measured employing X-ray tomography; a Zeiss XRADIA Versa XRM-500 system. The acceleration voltage was set to 50 kV, with a current of 79 µA. The exposure time of each projection was 1750 ms. The projection image of 1013 by 1013 pixels is described with a 16 bit grey level. A geometric magnification of 3.35 was achieved, and combined with the optical magnification of 4 yielded to a projected pixel size of 2 µm, using a pixel binning of 2. The volume was reconstructed over a grid of cubic voxels with a side length of the 2 µm. The data set generated with the XCT system was analysed in VG studio 3.0, Volume Graphics GmbH Heidelberg Germany. The surface model was created using VG's advanced surface determination, starting from an ISO 50 surface determination.

Two sets of blind holes were drilled. The first set was produced employing the 100 mm telecentric lens with 35 µm beam spot diameter and the holes' depth as a function of pulse numbers was analysed as shown in Figure 8. It can be seen that the "saturation" point was reached after 1000 pulses while the achieved depth was 115 µm. Considering the silicon nitride substrate thickness of 250 µm used in this research, this depth was not sufficient to penetrate it even by applying the two-side drilling method. The second set of blind holes was produced using the 50 mm focusing lens with 25 µm beam diameter and thus a higher fluence

was used. A higher depth at the saturation point was achieved, i.e. 150 µm, after delivering 1600 pulses. These process settings were used to validate the proposed two-side drilling method.

4.4 Design of experiments

4.4.1 In-process measurement uncertainty

As was stated in Section 3.5, before implementing the proposed in-process inspection methodology, the uncertainty associated with such measurements needs to be determined. The sources of type A uncertainties were identified and the following experiments were carried out to quantify them:

U1. and *U2*. To determine the uncertainty of measuring micro holes' coordinates in SCS, a single micro hole was produced by laser percussion drilling. The hole was scanned ten times with the R25 sensor and then the standard deviation of its coordinates was calculated.

U3. The uncertainty of measuring the entrance of a reference hole on one side of the sample was determined in the same way as U1 but a 500 µm diameter through hole produced by laser drilling was used.

U4. The exit side of the reference hole was measured ten times to determine the uncertainty in the same as U3.

U5. To access the uncertainty of correlating the SCSs on the two sides of the sample, 20 through holes were laser drilled as shown in Figure 9 and the distances between them were compared on both sides. To minimise the additional uncertainty due to this measurement, it

was carried out on the Alicona G5 system with 50× objective lens with higher lateral and vertical resolutions, i.e. 640 nm and 20 nm, respectively.

U6. The angular deviation of the A_{MCS} and X_{SCS} were measured ten times, and their standard uncertainty was computed based on the sensitivity coefficient and probability divisor.

The type A uncertainties, U1-U6, have been assumed to be of normal distribution with the divisor of 1; and a degree of freedom (DoF) of $n-1$, where n is the number of samples. The sensitivity coefficient of the uncertainties has been taken as one, except for U6 for which the uncertainty of detecting the angular displacement between the A_{MCS} and X_{SCS} axes is a geometric function of the angle and the field of view of the sensor. Given that the angle is small, the sensitivity coefficient for the maximum displacement can be assumed based on the maximum field of view of the sensor.

U7. Given the digital readout of the resolution of the C_{MCS} axis, the probability distribution of the resolution has been assumed to be rectangular, with a divisor of $\sqrt{3}$, and DoF of infinity.

After finding the standard uncertainty of all the steps associated with the proposed in-process alignment measurement method, its combined uncertainty was calculated using the root-square-sum of the standard uncertainties as follows:

$$U_c = \sqrt{(U1)^2 + (U2)^2 + (U3)^2 + (U4)^2 + (U5)^2 + (U6)^2 + (U7)^2} \quad (16)$$

The effective DoF has been calculated as 41, using the Welch-Satterthwaite formula. This effective DoF yields to a k-factor of 1.93 at a 97% confidence level. Hence the expanded uncertainty, U, can be stated as:

$$U = k.U_c \quad (17)$$

4.4.2 Hole alignment accuracy

Considering the measurement uncertainty associated with the proposed in-process inspection method, it would be possible to verify the alignment accuracy of holes produced employing the two-side drilling method. In particular, 10 pairs of holes were produced on two opposite sides of a sample and their alignment accuracy was measured with the in-process inspection method. The holes' positions were selected in different areas within the working envelope of the laser processing setup and thus to consider the worst-case scenario in assessing the achievable alignment accuracy.

4.4.3 Hole morphology

Micro holes with different cross-sections were produced by employing both the one-side and the proposed two-side drilling methods. A test sample was designed, as shown in Figure 10, to compare their capabilities. It includes 4 arrays of holes:

Array A: The holes in each row were produced employing percussion drilling from one side with the laser settings selected in Section 4.3. The only difference between the rows was the number of pulses used as stated in Figure 10.

Array B: The same as Array A but percussion drilling from two sides was employed. Again, the pulse numbers were varied to see how the holes evolved before and after reaching the substrate depth with 1600 pulses.

Array C: Holes with nominal square and circular cross-sections were produced employing a drilling strategy that involved layer based hatching with the laser beam by changing the hatching direction 45^0 at each layer. The hatching distance was set on 4μm and the hole edges were outlined at each layer. By using this strategy the holes on one side were drilled using again the laser settings selected in Section 4.3. The holes in each row are identical and the sizes and cross-sections were varied as shown in Figure 10.

Array D: The same as Array C but produced employing the two-side processing method.

All four holes' arrays were measured with the XCT system and the hole sizes and shapes in different cross sections were compared.

5. Results and discussion

5.1. In-process measurement uncertainty

The different sources of uncertainty were assessed experimentally as described in Section 3.4.2 and thus to calculate the expanded uncertainty associated with the proposed in-process inspection method. The results are provided in Table 1. It can be seen that the greatest uncertainty contribution was U6 which depends on both the lateral and vertical resolutions of the R25 sensor. To minimise U6 the R25 resolution can be increased by using higher magnification objectives but this will reduce the sensor field of view. As a consequence, it may be required to "stitch" fields with the associated uncertainty with this and also the time necessary to execute in-process inspection routines will increase. U1 to U5 are directly dependent on the geometrical accuracy of the laser drilled holes and their edge definition. For example, it is clear from the values of U3 and U4 that the edge definition of the reference hole entrance is worse than its exit due to the laser drilling side effects. Hence, the contributions of U1 to U5 can be reduced by optimising further the laser drilling settings. The expanded uncertainty calculated using Eq. (16) and (17) is 0.9 µm with a confidence level of 97%. This is in line with the requirements stated in Section 3.2.4, i.e. the uncertainty associated with the proposed in-process measurement routines to be within a fifth of required positional accuracy of the drilled holes (in the range from 5 to 10 µm).

5.2 Hole alignment accuracy

The statistical results obtained by using R25 sensor to assess the alignment accuracy of 10 pair of holes with the proposed in-process measurement method are: Min: 1.22 µm, Max: 8.33 µm, Average: 4.46 µm and Standard Deviation: 2.52 µm. These variations in the achieved alignment accuracy are mainly due to errors associated with the edge detection by using the chromatic confocal sensor and can be minimised by optimising the laser parameter setting for producing the through reference holes and by choosing a chromatic confocal sensor with a higher resolution. However, there are trade-offs as a higher resolution sensors entail shorter working distances and hence impact on the flexibility of the alignment procedure and increase the possibilities for collisions. Another reason for these variations is the resolution and repeatability of mechanical stages that can be improved by selecting stages with higher resolution and/or precision.

Taking into account the measurement uncertainty, it can be stated that the misalignment between the entrances and exits of through holes produced with the proposed two-side laser drilling method is better than (8.3 ± 0.9) µm.

5.3. Hole morphology

The hole morphology was analysed with the XCT system. The cross sections of hole arrays (see Figure 10) produced by percussion drilling are shown in Figure 11. The evolution of the holes and the way the pairs of holes meet when the two-side drilling method is applied are shown in Figure 11b. It can be seen that the entrance and exit holes' diameters are approximately identical. Comparing the results in Figure 11c it is apparent that the through holes that were not possible to produce with the one-side method were drilled successfully

with the proposed two-side method. In addition, as can be seen in Figure 11a good repeatability can be achieved in producing holes with 2500 pulses employing the two-side method. The evolutions of holes' diameters with the increase of pulse numbers are shown in Figure 12 and Figure 13 for one- and two-side drilling methods, respectively. There are only marginal differences in the morphology of the holes drilled with 5000 and 7500 pulses from one-side, which shows again that the saturation point is already reached at these pulse numbers. Considering the holes' evolution in the two-side drilling method, 200, 400 and 800 pulses were not sufficient to penetrate the sample while at 1600 pulses the hole shape has started to emerge and then to arrive at the final shape of the holes at 2500 pulses. A further increase of pulse number, i.e. 5000 and 7500 pulses, leads to only marginal changes, i.e. a slight increase of exit diameter while the necking diameter decreases. Thus, the results are quite conclusive in regards to the optimum number of pulses necessary to produce through holes in the 250 µm silicon nitride substrate with the two-side drilling method.

The holes' cross sections of arrays C and D (see Figure 10) resulting from the use of a different drilling strategy from one- and two sides are depicted in Figure 14. Again good repeatability is achieved with the two-side drill method in producing 60 µm rectangular holes (Figure 14a). The tapering effect in drilling the holes from one-side is very pronounced in Figure 14c while it is almost negligible in the two-side approach (Figure 14b). The evolutions of holes' sizes with the increase of pulse numbers in both drilling approaches provided in Figure 15 and Figure 16 also shows clearly the resulting differences in regards to the tapering effects.

In addition, the deviations from holes' geometrical accuracy in both drilling methods, i.e. roundness and tapering angle in producing 75 µm holes, are depicted in Figure 17. Although the outer hole diameter is bigger when the two-side drilling is used, the average circularity of the holes is still better. For example, the roundness deviation of the three cross sections

shown in Figure 17 decreased when the two-side approach was used while the holes' profile was much closer to the circular shape in all three cross-sections. The circularity of the holes' exits is almost the same for two-side and one-side drilling (8.5μm and 8.9μm respectively), however holes' diameters and profiles are quite different and only in the two-side drilling method are close to the hole target size and form, i.e. cylindricity.

6. Conclusion

In this paper, a new two-side drilling method is proposed. A pilot two-side laser processing setup was designed and for its implementation the following enabling tools and technologies were developed and validated:

- A specially designed laser processing setup that integrates two rotary and three linear mechanical stages together with a modular workpiece holding device to ensure the required motion control, accuracy and repeatability in executing two-side laser processing routines;
- System level tools for fully automated process setting up that allow errors from various sources to be compensated and thus to minimise their impact on achievable accuracy and repeatability in two-side laser processing;
- A fully automated laser processing method for drilling holes with high alignment accuracy and repeatability from two opposite sides;
- A method for fully automated correlation of working coordination systems in two-side laser processing;
- In-process inspection method for verifying the alignment accuracy achievable with the proposed two-side laser processing method.

The new two-side drilling method was validated experimentally and the following conclusions can be made based on the obtained results.

- The achievable alignment accuracy of through holes with different cross-sections produced with the proposed two-side drilling method is better than 10 µm. It is important to note that this accuracy can be improved by optimising the laser parameter settings and also by employing a higher accuracy and resolution stages and sensors for process setting up.
- Micro holes with very good repeatability and dimensional and geometrical accuracy were produced by two-side drilling that cannot be achieved employing one-side drilling.
- The achievable aspect ratios can be more than doubled in comparison with the one-side drilling method while improving the holes' dimensional and geometrical accuracy.

In addition, it is worth mentioning the application area of the proposed method can be broaden to two-side drilling of workpiece with not parallel surfaces, e.g. for drilling intersecting holes and micro channels inside components for fluid flow and heat exchange applications.

Acknowledgments

The research reported in this paper was supported by Korea Institute for Advancement of Technology (KIAT), i.e. the project on "Laser Machining of Ceramic Interface Cards for 3D wafer bumps", European Commission H2020 FoF programme, i.e. the project on "Modular laser based additive manufacturing platform for large scale industrial applications" (MAESTRO), and the Engineering and Physical Sciences Research Council (EPSRC Grants EP/M008983/1 and EP/L01534X/1). The authors would like to thank Alicona Imaging

GmbH for their support and advice in implementing the in-process measurement method reported in this paper and also to acknowledge the contribution of Martin Corfield in carrying out the XCT measurements.

NOMENCLATURE

$\Delta\alpha$	Angular displacements of the incident beam from the workpiece surface normal in regards to the A axis.
$\Delta\beta$	Angular displacements of the incident beam from the workpiece surface normal in regards to the B axis.
$\Delta\psi$	Perpendicularity displacement of incident beam and the A axis.
$\Delta\gamma$	Angular displacements of X_{MCS} and A_{MCS}.
ΔX_A	Axial displacements of the stage in X direction after executing a rotation by 180°.
$\Delta\vartheta$	Angular displacement of the stage after a rotation by 180° with the A stage.
a	The slope of A_{MCS} in $X_{MCS}Y_{MCS}$ plane.
b	Y intercept of A_{MCS} axis in $X_{MCS}Y_{MCS}$ plane.
X, Y	Hole's coordinates in MCS on first side.
X_{new}, Y_{new}	Hole's coordinates in MCS on second side.
$\Delta\emptyset$	Angular displacement between A_{MCS} and X_{SCS}.
E_X, E_Y	Misalignment of a hole in X_{SCS} and Y_{SCS} directions.
E	Total misalignment of a hole.

n	Number of samples used to estimate standard uncertainty.
DoF	Degree of freedom.
U_c	Combined uncertainty.
k	K-factor for estimating expanded uncertainty.
U	Expanded uncertainty.
M^2	Beam quality factor.

References

1. Özel, T., *Editorial: Special section on micromanufacturing processes and applications.* Materials and Manufacturing Processes, 2009. **24**(12): p. 1235.
2. Chavoshi, S.Z. and X. Luo, *Hybrid micro-machining processes: A review.* Precision Engineering, 2015. **41**: p. 1-23.
3. Luo, X., et al., *Design of ultraprecision machine tools with applications to manufacture of miniature and micro components.* Journal of Materials Processing Technology, 2005. **167**(2-3): p. 515-528.
4. Leo Kumar, S.P., et al., *A review on current research aspects in tool-based micromachining processes.* Materials and Manufacturing Processes, 2014. **29**(11-12): p. 1291-1337.
5. Al-Ahmari, A.M.A., et al., *A Hybrid Machining Process Combining Micro-EDM and Laser Beam Machining of Nickel-Titanium-Based Shape Memory Alloy.* Materials and Manufacturing Processes, 2016. **31**(4): p. 447-455.
6. Dandekar, C.R., Y.C. Shin, and J. Barnes, *Machinability improvement of titanium alloy (Ti–6Al–4V) via LAM and hybrid machining.* International Journal of Machine Tools and Manufacture, 2010. **50**(2): p. 174-182.
7. Adelmann, B. and R. Hellmann, *Rapid micro hole laser drilling in ceramic substrates using single mode fiber laser.* Journal of Materials Processing Technology, 2015. **221**: p. 80-86.
8. Choi, W.C. and J.Y. Ryu, *Fabrication of a guide block for measuring a device with fine pitch area-arrayed solder bumps.* Microsystem Technologies, 2012. **18**(3): p. 333-339.
9. Watanabe, N., et al., *Fabrication of a membrane probe card using transparent film for three-dimensional integrated circuit testing.* Japanese Journal of Applied Physics, 2014. **53**(6 SPEC. ISSUE).
10. Choi, W.C. and J.Y. Ryu, *A MEMS guide plate for a high temperature testing of a wafer level packaged die wafer.* Microsystem Technologies, 2011. **17**(1): p. 143-148.
11. Huang, H., L.-M. Yang, and J. Liu, *Micro-hole drilling and cutting using femtosecond fiber laser.* Optical Engineering, 2014. **53**(5).
12. Lim, H.S., et al., *A study on the machining of high-aspect ratio micro-structures using micro-EDM.* Journal of Materials Processing Technology, 2003. **140**(1–3): p. 318-325.
13. Wang, X.C., et al., *Femtosecond laser drilling of alumina ceramic substrates.* Applied Physics a-Materials Science & Processing, 2010. **101**(2): p. 271-278.
14. Khan, A.H., et al., *Influence of microsupersonic gas jets on nanosecond laser percussion drilling.* Optics and Lasers in Engineering, 2007. **45**(6): p. 709-718.
15. Khan, A.H., et al., *Numerical analysis of gas-dynamic instabilities during the laser drilling process.* Optics and Lasers in Engineering, 2006. **44**(8): p. 826-841.
16. Hsu, J.C., et al., *Continuous-wave laser drilling assisted by intermittent gas jets.* International Journal of Advanced Manufacturing Technology, 2015. **79**(1-4): p. 449-459.
17. Ho, C.C., et al., *Characteristics of the effect of swirling gas jet assisted laser percussion drilling based on machine vision.* Journal of Laser Applications, 2015. **27**(4).
18. Li, Q.K., et al., *Sapphire-Based Dammann Gratings for UV Beam Splitting.* IEEE Photonics Journal, 2016. **8**(6).
19. Juodkazis, S., et al., *Laser-Induced Microexplosion Confined in the Bulk of a Sapphire Crystal: Evidence of Multimegabar Pressures.* Physical Review Letters, 2006. **96**(16): p. 166101.
20. Lott, G., et al., *Optimizing the processing of sapphire with ultrashort laser pulses.* Journal of Laser Applications, 2016. **28**(2).
21. Zhang, H., et al., *An investigation on the hole quality during picosecond laser helical drilling of stainless steel 304.* Applied Physics a-Materials Science & Processing, 2015. **119**(2): p. 745-752.
22. Zhang, Y., et al., *Micromachining features of TiC ceramic by femtosecond pulsed laser.* Ceramics International, 2015. **41**(5): p. 6525-6533.

23. Tokarev, V.N., et al., *Optimization of plasma effect in laser drilling of high aspect ratio microvias.* Laser Physics, 2015. **25**(5).
24. Penchev, P., V. Nasrollahi, and S. Dimov, *Laser micro-machining method for producing high aspect ratio features*, in *11th International Conference on Micro Manufacturing ICOMM*. 2016: Orange County, California, USA.
25. Nasrollahi, V., P. Penchev, and S. Dimov, *A new laser drilling method for producing high aspect ratio micro through holes*, in *4M/IWMF Conference*. 2016: Lyngby, Denmark.
26. Penchev, P., et al., *Novel Manufacturing Route for Scale Up Production of Terahertz Technology Devices.* Journal of Micro and Nano-Manufacturing, 2016. **4**(2): p. 021002-021002.
27. Wang, G.Q., et al., *Investigation of the hole-formation process during double-sided through-mask electrochemical machining.* Journal of Materials Processing Technology, 2016. **234**: p. 95-101.
28. Goya, K., et al., *Efficient deep-hole drilling by a femtosecond, 400 nm second harmonic Ti:Sapphire laser for a fiber optic in-line/pico-liter spectrometer.* Sensors and Actuators B-Chemical, 2015. **210**: p. 685-691.
29. VanderWert, T.L., *Laser processing aircraft and turbine engine parts.* 1993 SAE Aerospace Atlantic Conference and Exposition, 1993.
30. Sivarao, et al., *Establishing a hybrid laser lathing technology.* World Applied Sciences Journal, 2013. **21**(SPECIAL ISSUE2): p. 53-59.
31. Ocaña, J.L., et al., *Micromachining of 2D-3D structures with high intensity laser pulses.* Journal of Optoelectronics and Advanced Materials, 2011. **13**(8): p. 976-980.
32. Kawamura, Y., A. Kai, and K. Yoshii, *Various kinds of pulsed ultraviolet laser micromachinings using a five axis microstage.* Journal of Laser Micro Nanoengineering, 2010. **5**(2): p. 163-168.
33. Jin, S.Y., K.T. Lee, and K. Kim, *Volumetric error compensation of multi-axis laser machining center for direct patterning of flat panel display.* Journal of Manufacturing Science and Engineering, Transactions of the ASME, 2006. **128**(1): p. 239-248.
34. Bhaduri, D., et al., *An investigation of accuracy, repeatability and reproducibility of laser micromachining systems.* Measurement: Journal of the International Measurement Confederation, 2016. **88**: p. 248-261.
35. Kim, K., et al. *Laser scanner stage on-the-fly method for ultrafast and wide area fabrication*. in *6th International WLT Conference on Lasers in Manufacturing, LiM*. 2011. Munich.
36. Penchev, P., et al., *Generic software tool for counteracting the dynamics effects of optical beam delivery systems.* Proceedings of the Institution of Mechanical Engineers, Part B: Journal of Engineering Manufacture, 2015: p. 1-17.
37. Penchev, P., S. Dimov, and D. Bhaduri, *Experimental investigation of 3D scanheads for laser micro-processing.* Optics & Laser Technology, 2016. **81**: p. 55-59.
38. Penchev, P., et al., *Generic integration tools for reconfigurable laser micromachining systems.* Journal of Manufacturing Systems, 2016. **38**: p. 27-45.
39. Ramesh, R., M.A. Mannan, and A.N. Poo, *Error compensation in machine tools — a review: Part I: geometric, cutting-force induced and fixture-dependent errors.* International Journal of Machine Tools and Manufacture, 2000. **40**(9): p. 1235-1256.
40. Schwenke, H., et al., *Geometric error measurement and compensation of machines—An update.* CIRP Annals - Manufacturing Technology, 2008. **57**(2): p. 660-675.
41. Schmitt, R., et al., *Inline Process Metrology System for the Control of Laser Surface Structuring Processes.* Physics Procedia, 2012. **39**: p. 814-822.
42. *Evaluation of measurement data.* Guide to the Expression of Uncertainty in Measurement, 2008.
43. Dergez, D., et al., *Mechanical and electrical properties of DC magnetron sputter deposited amorphous silicon nitride thin films.* Thin Solid Films, 2015. **589**: p. 227-232.

44. Artigas, R., *Imaging Confocal Microscopy*, in *Optical Measurement of Surface Topography*, R. Leach, Editor. 2011, Springer Berlin Heidelberg: Berlin, Heidelberg. p. 237-286.
45. Chen, C.-N. and J.-J. Huang, *Characteristics of thin-film transistors based on silicon nitride passivation by excimer laser direct patterning.* Thin Solid Films, 2013. **529**: p. 449-453.
46. Poulain, G., et al., *Laser Ablation Mechanism Of Silicon Nitride Layers In A Nanosecond UV Regime.* Energy Procedia, 2012. **27**: p. 516-521.
47. Ho, C.Y. and J.K. Lu, *A closed form solution for laser drilling of silicon nitride and alumina ceramics.* Journal of Materials Processing Technology, 2003. **140**(1–3): p. 260-263.
48. Atanasov, P.A., E.D. Eugenieva, and N.N. Nedialkov, *Laser drilling of silicon nitride and alumina ceramics: A numerical and experimental study.* Journal of Applied Physics, 2001. **89**(4): p. 2013-2016.

Figure Captions List

Fig. 1 Angular displacements of incident beam and: (a) workpiece normal in regards to the A axis, $\Delta\alpha°$; (b) workpiece normal in regards to the B axis, $\Delta\beta°$ (c) A axis, $\Delta\psi°$.

Fig. 2 Required adjustments in X and Y directions (*dx, dy*) due to: (a) displacement of holes' positions in respect to the A axis; and (b) the A axis not being parallel to the X axis, $\Delta\gamma°$.

Fig. 3 Required compensational movements in Z direction due to displacements between A axis and the centre plane of the workpiece, ΔZ

Fig. 4 The setting up procedure for determining initial coordinates of two through holes centres (Points 5, 6) and them their corresponding coordinates (points 7, 8 respectively) after a rotation by 180^0

Fig. 5 In-process inspection method with a 3D metrology sensor: (a) the first side field of view and (b) the second side field of view

Fig. 6 Three views of the used laser processing setup: (a) confocal sensor; (b) the focusing lens together with the stack of mechanical stages; (c) the R25 sensor

Fig. 7 The specially designed modular work holding device

Fig. 8 Determining the optimum numbers of pulses with two different lenses

Fig. 9 The array of holes used to evaluate uncertainty in correlating SCSs on the sample two sides

Fig. 10 The test sample designed to compare one- and two-side drilling methods

Fig. 11 Holes' cross-sections generated using the XCT system: (a) section G-G of holes' array B produced by two-side drilling with 2500 pulses; (b) section H-H of holes' array B produced by two-side drilling with different pulse numbers; (c) section I-I of holes' array A produced by one-side drilling with different pulse numbers

Fig. 12 Morphology analysis of holes produced employing one-side percussion drilling with different pulse numbers

Fig. 13 Morphology analysis of holes produced employing two-side percussion drilling with different pulse numbers

Fig. 14 Holes' cross-sections generated using the XCT system: (a) section J-J of 60µm square holes (Array D) produced by two-side drilling; (b) section K-K of square and circular holes with different dimensions (Array D) produced by two-side drilling; (c) section L-L of square and circular holes with different dimensions (Array C) produced by one-side drilling.

Table Captions List

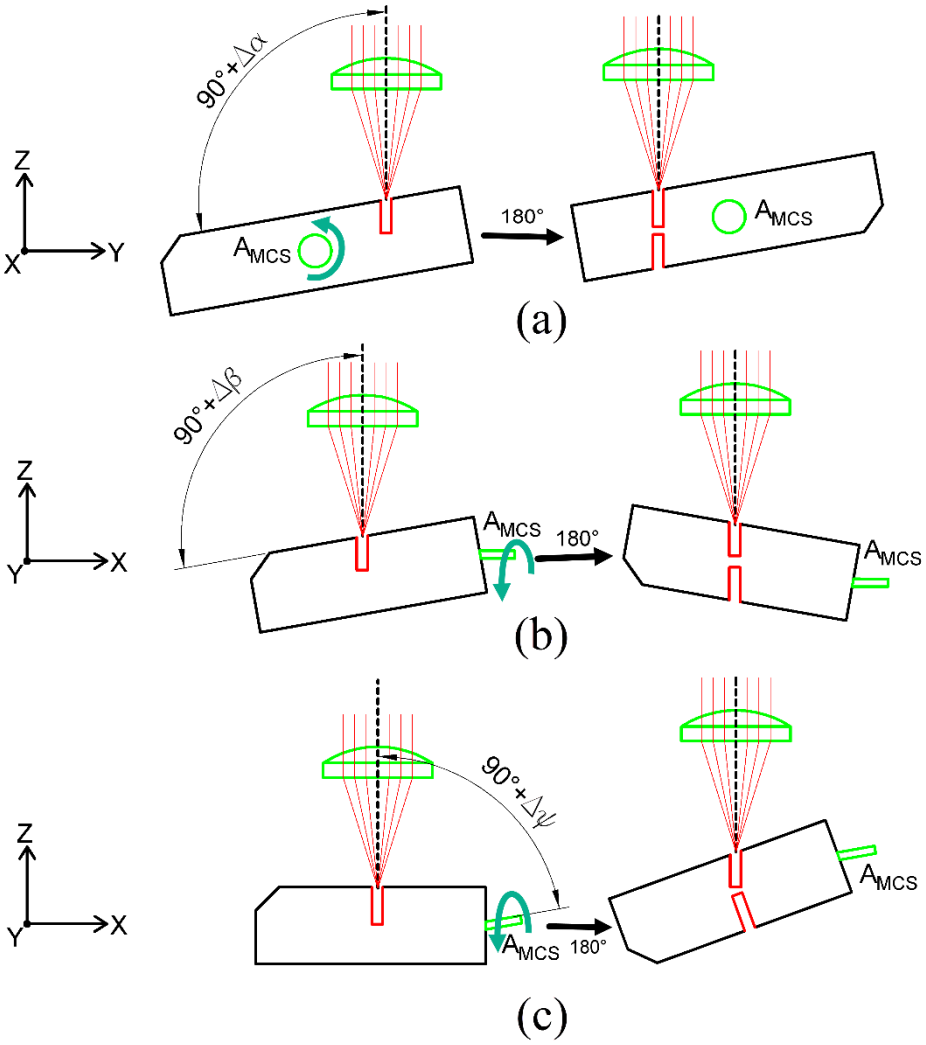

Figure 1. Angular displacements of incident beam and: (a) workpiece normal in regards to the A axis, $\Delta\alpha$°; (b) workpiece normal in regards to the B axis, $\Delta\beta$° (c) A axis, $\Delta\psi$°.

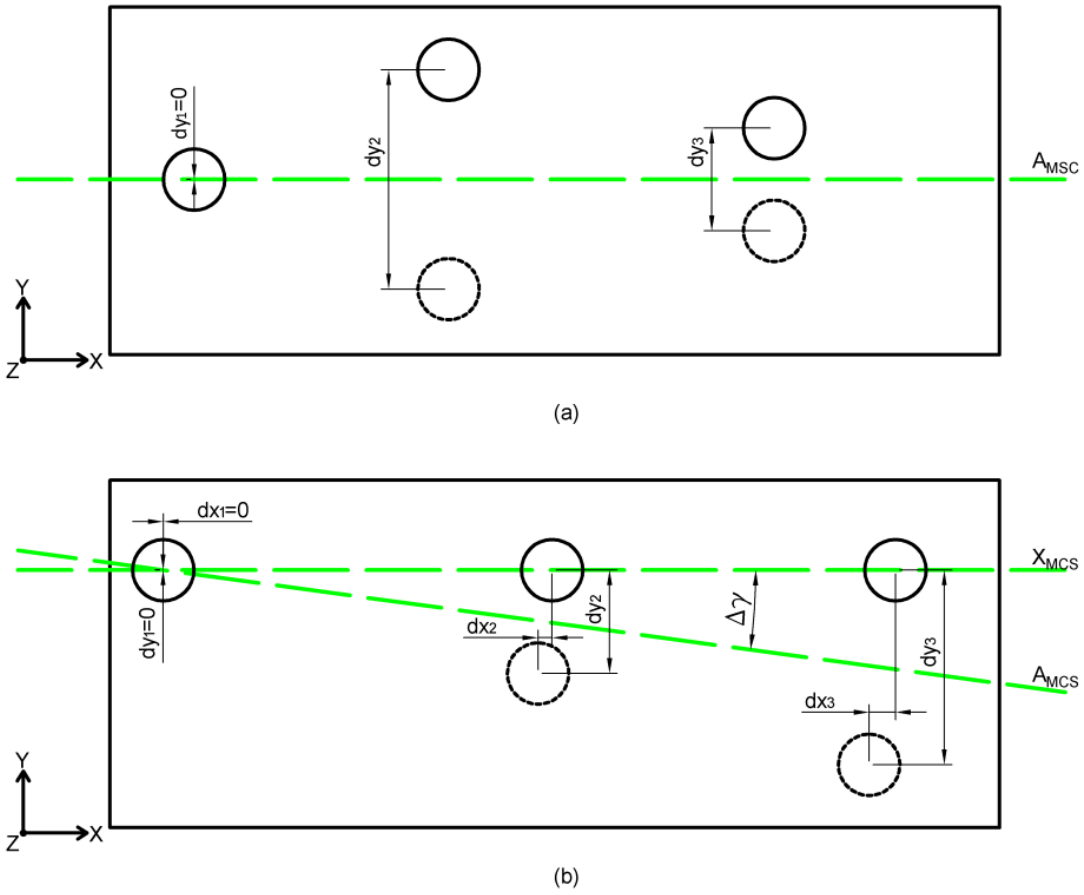

Figure 2. Required adjustments in X and Y directions (*dx*, *dy*) due to: (a) displacement of holes' positions in respect to the A axis; and (b) the A axis not being parallel to the X axis, $\Delta\gamma°$.

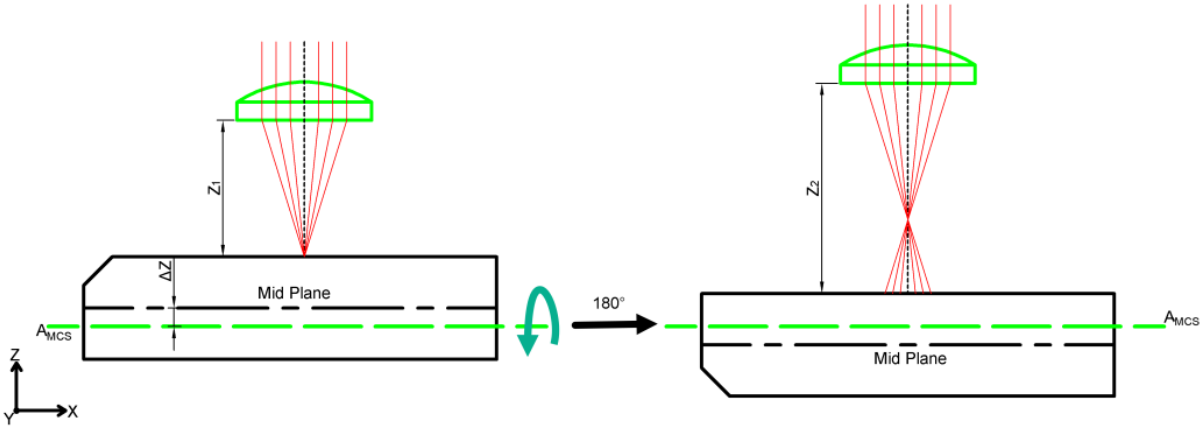

Figure 3. Required compensational movements in Z direction due to displacements between A axis and the centre plane of the workpiece, ΔZ

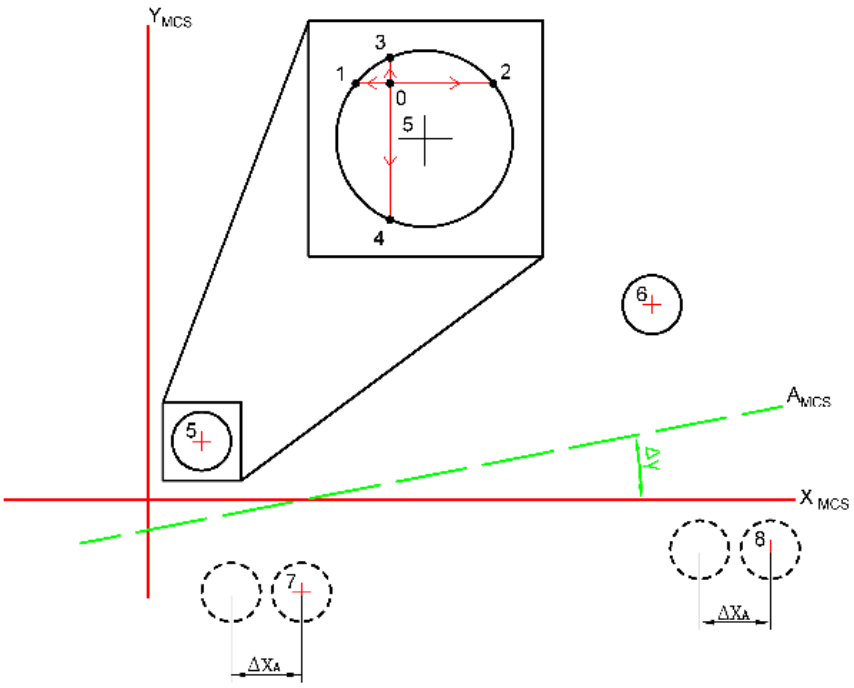

Figure 4. The setting up procedure for determining initial coordinates of two through holes centres (Points 5, 6) and them their corresponding coordinates (points 7, 8 respectively) after a rotation by 180^0

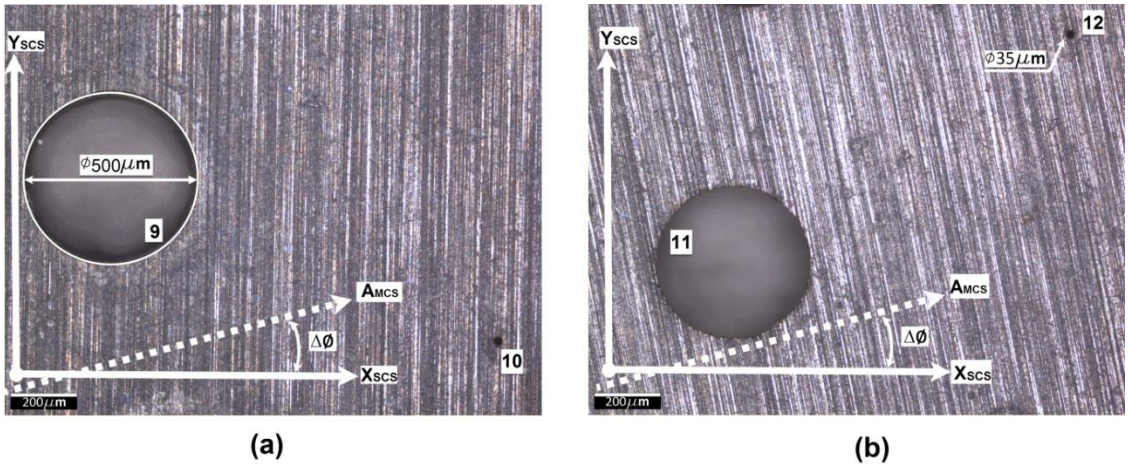

Figure 5. In-process inspection method with a 3D metrology sensor: (a) the first side field of view and (b) the second side field of view

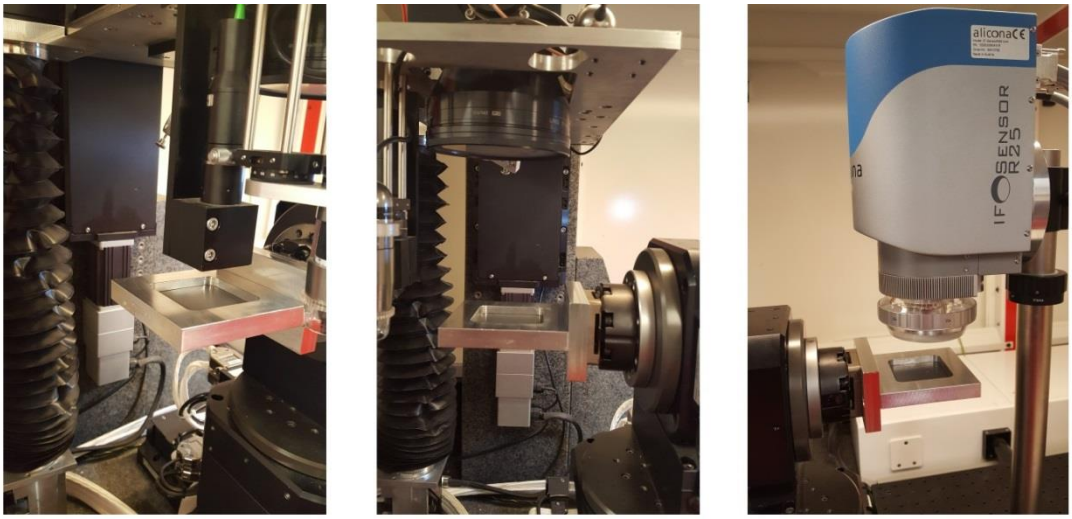

Figure 6. Three views of the used laser processing setup: (a) confocal sensor; (b) the focusing lens together with the stack of mechanical stages; (c) the R25 sensor

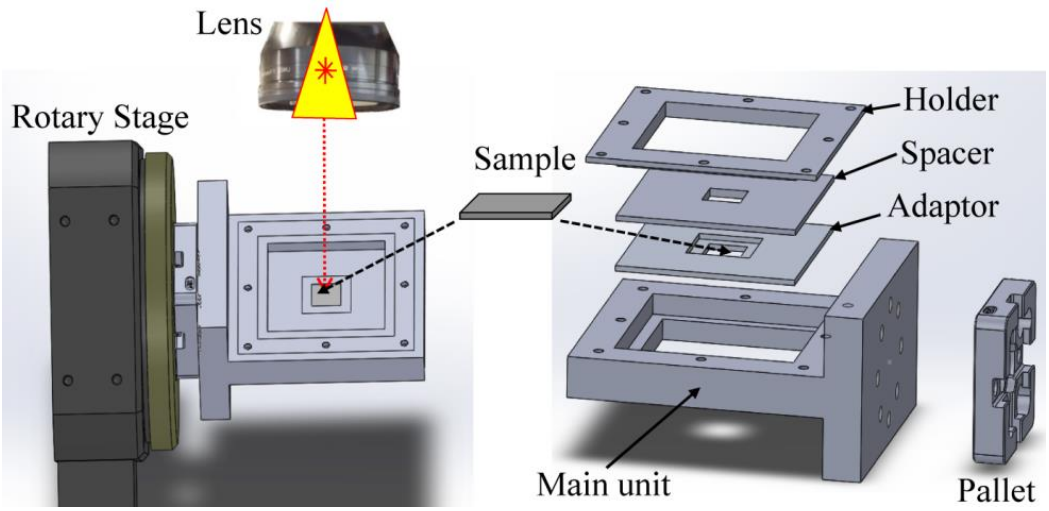

Figure 7. The specially designed modular work holding device

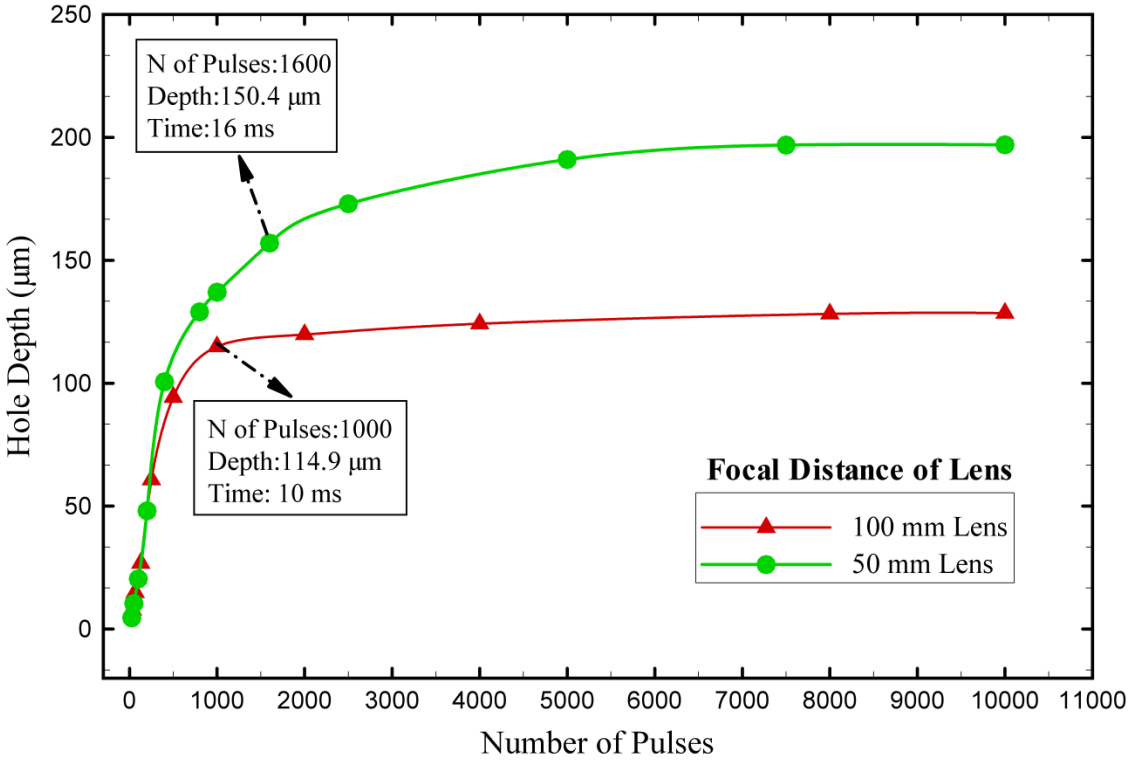

Figure 8. Determining the optimum numbers of pulses with two different lenses

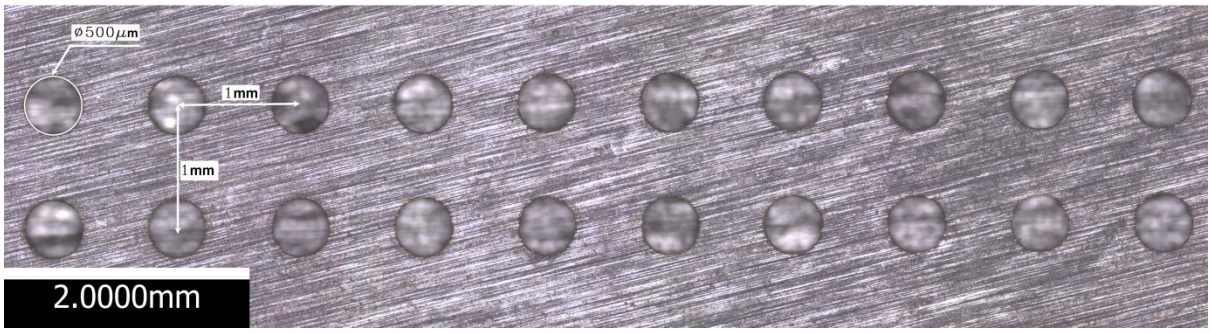

Figure 9. The array of holes used to evaluate uncertainty in correlating SCSs on the sample two sides

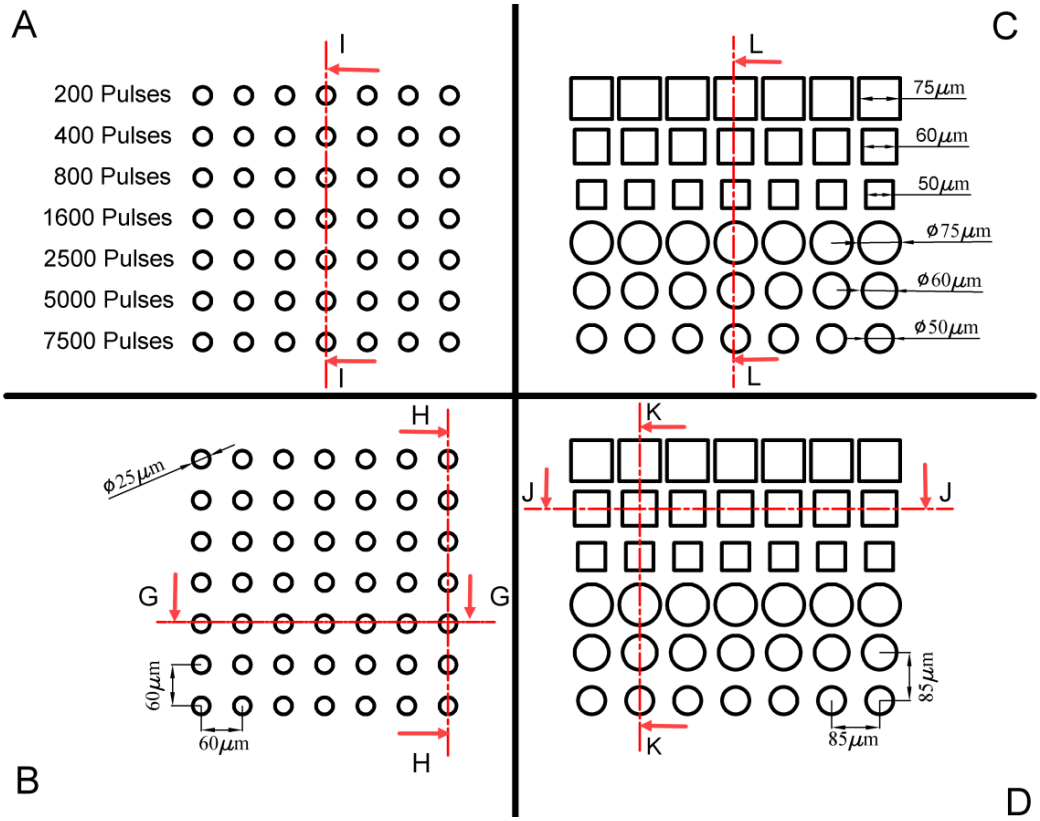

Figure 10. The test sample designed to compare one- and two-side drilling methods

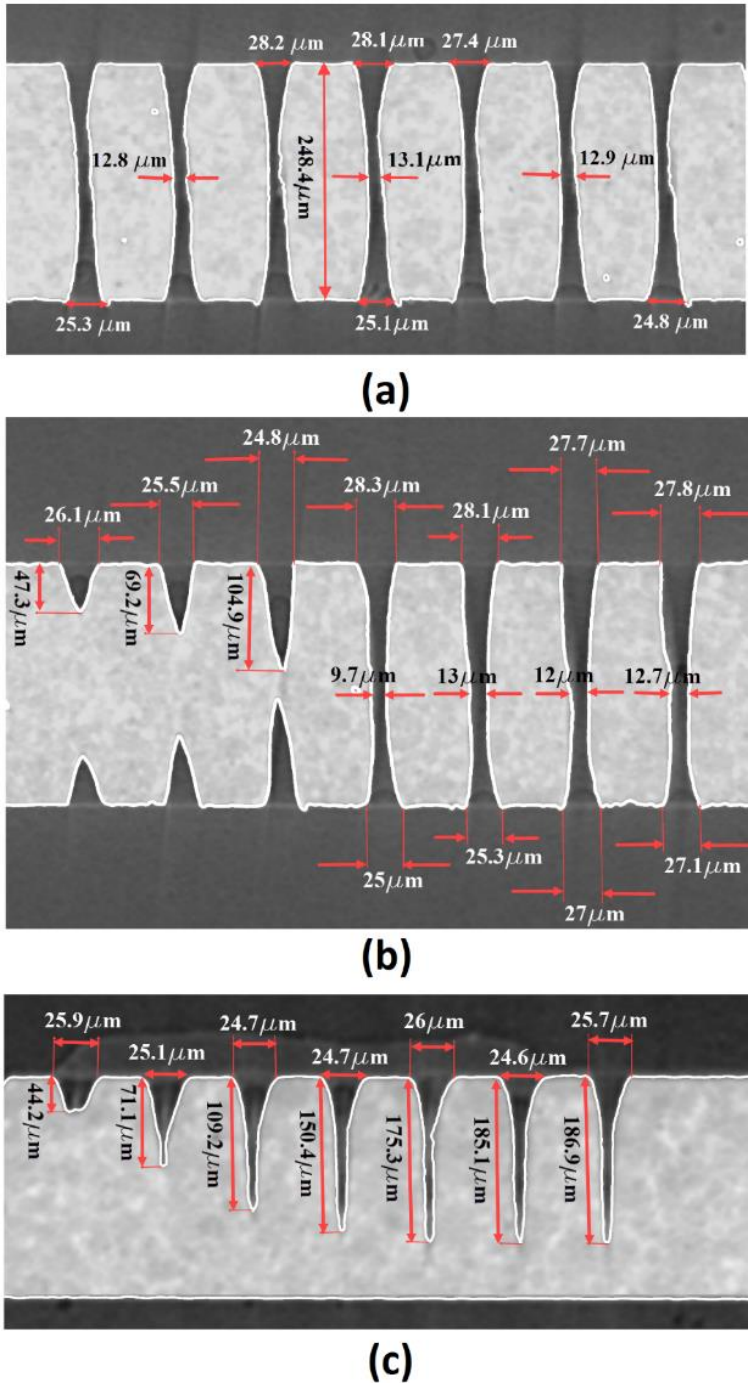

Figure 11. Holes' cross-sections generated using the XCT system: (a) section G-G of holes' array B produced by two-side drilling with 2500 pulses; (b) section H-H of holes' array B produced by two-side drilling with different pulse numbers; (c) section I-I of holes' array A produced by one-side drilling with different pulse numbers

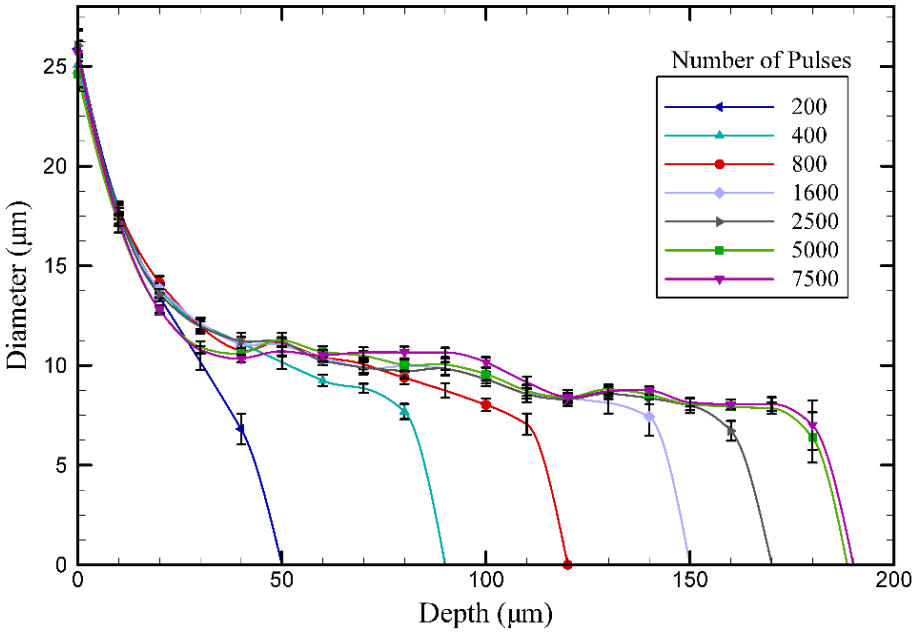

Figure 12. Morphology analysis of holes produced employing one-side percussion drilling with different pulse numbers

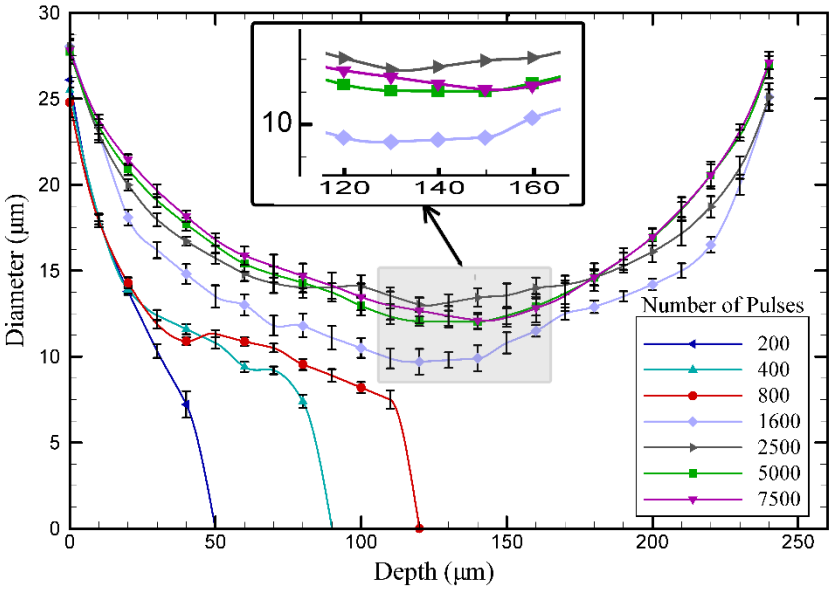

Figure 13. Morphology analysis of holes produced employing two-side percussion drilling with different pulse numbers

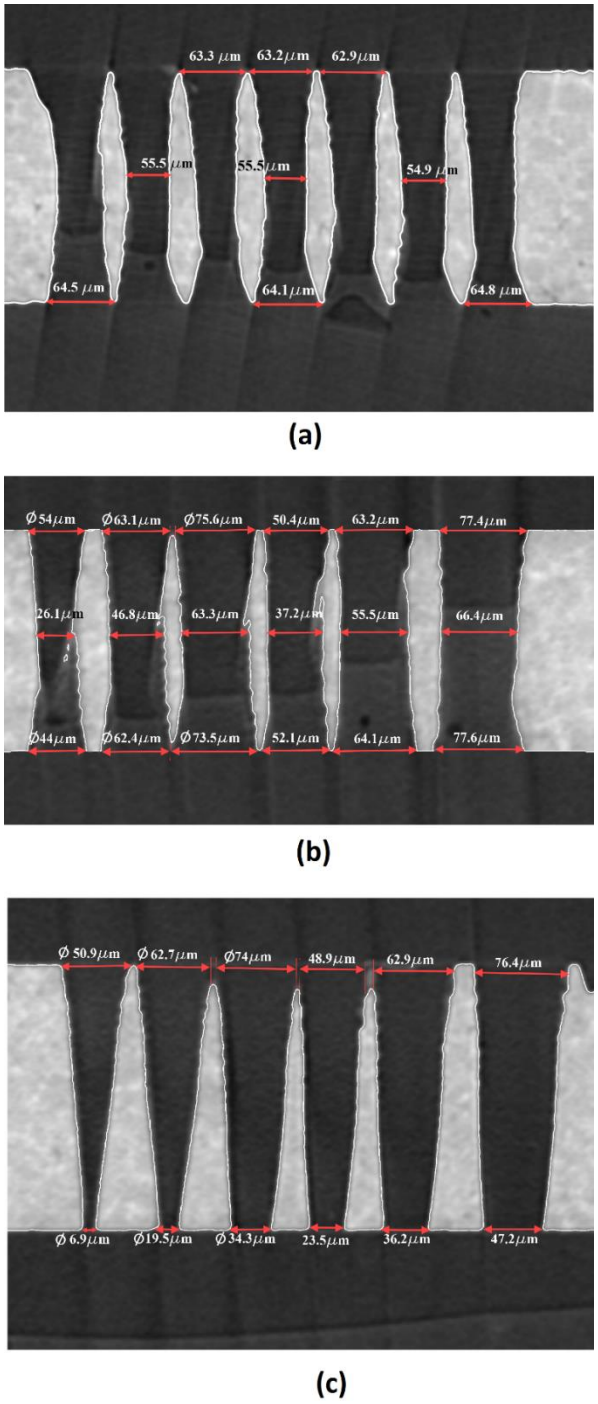

Figure 14. Holes' cross-sections generated using the XCT system: (a) section J-J of 60μm square holes (Array D) produced by two-side drilling; (b) section K-K of square and circular holes with different dimensions (Array D) produced by two-side drilling; (c) section L-L of square and circular holes with different dimensions (Array C) produced by one-side drilling.

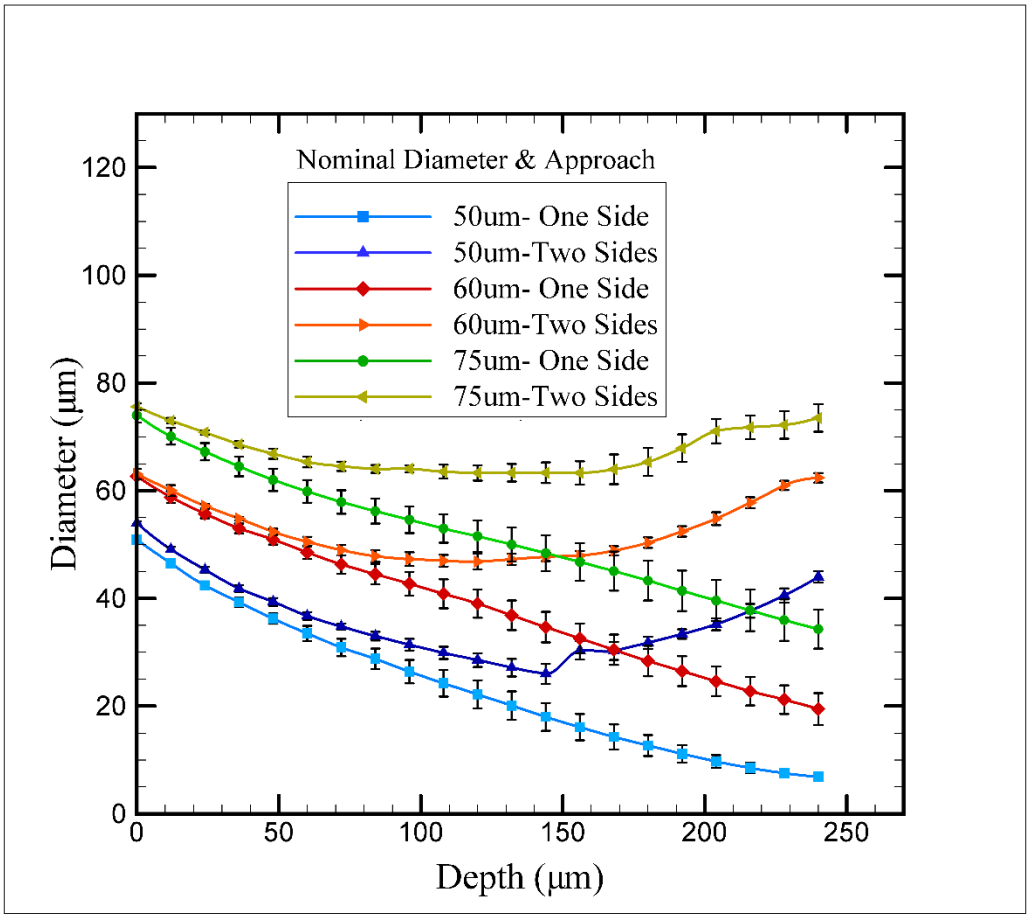

Figure 15. Morphology analysis of circular holes (arrays C and D) produced employing one- and two-side drilling

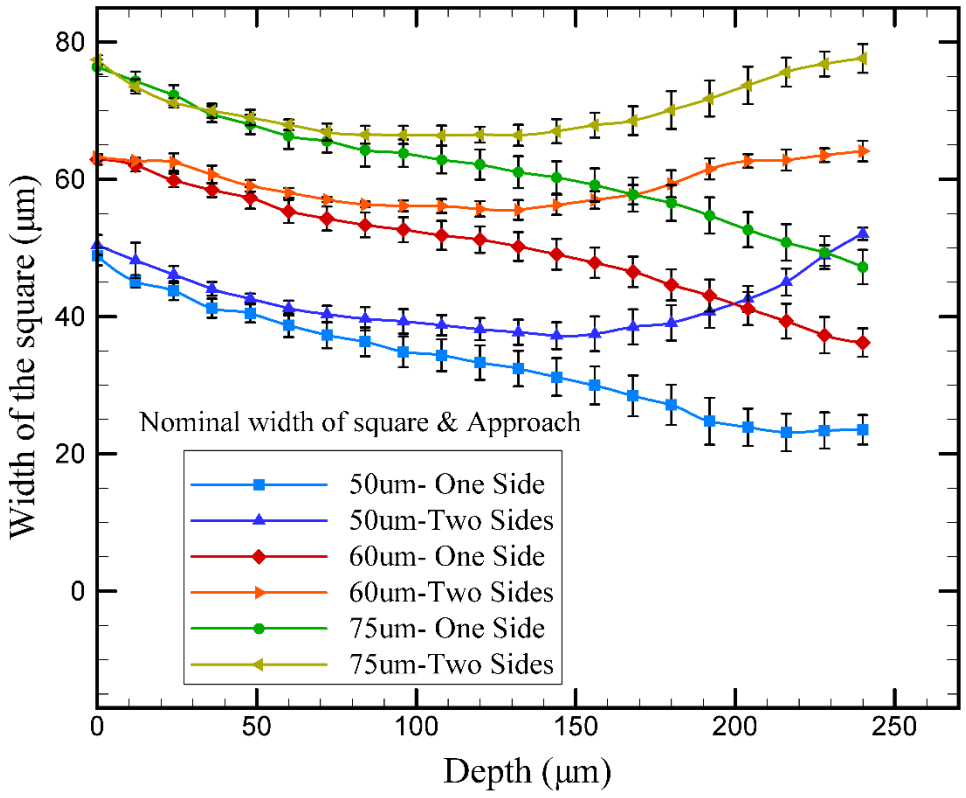

Figure 16. Morphology analysis of square holes (Arrays C and D) produced employing one- and two-side drilling

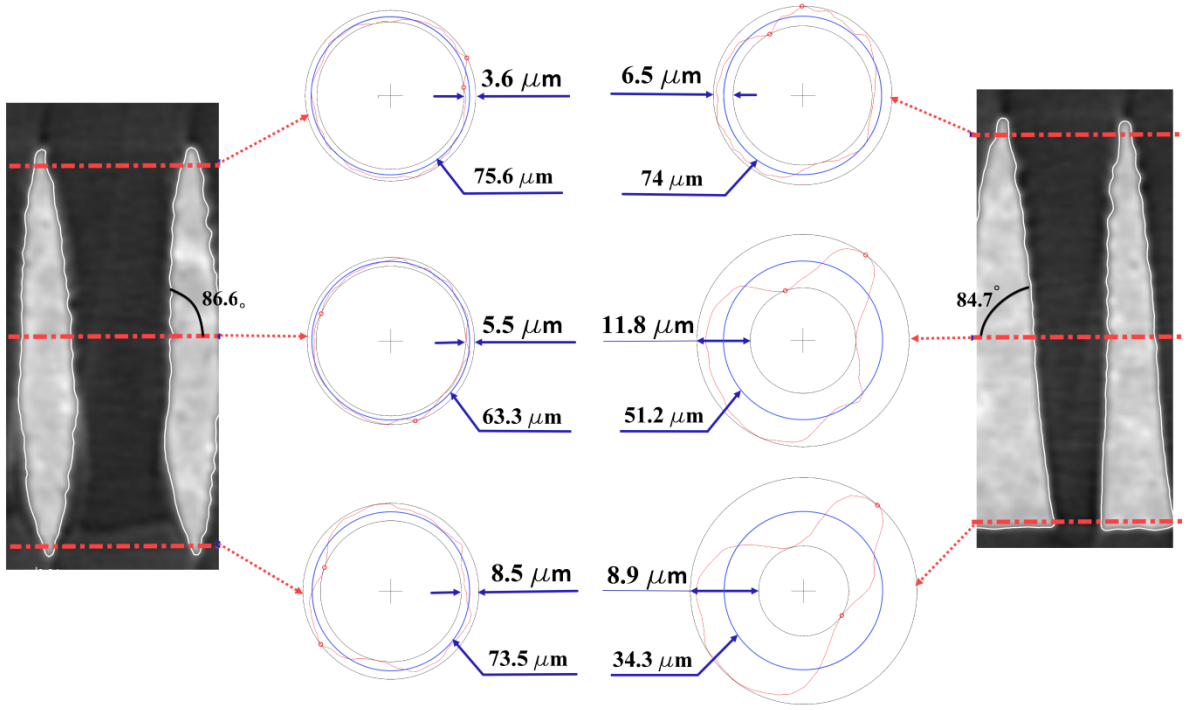

Figure 17. Roundness and tapering angles of 75μm circular holes (arrays C and D) produced by one- and two-side drilling

Table 1. The uncertainty budgets allocated to different error sources in performing in-process alignment measurements

	Uncertainty Source	Standard Uncertainty (μm)
U1	Measuring the micro hole centre in SCS	0.129
U2	Measuring the micro hole centre in SCS, second side	0.129
U3	Measuring the reference hole entrance in SCS	0.211
U4	Measuring the reference hole exit in SCS	0.096
U5	Correlating SCSs on the two sides	0.225
U6	Detecting the angular displacement between the A_{MCS} and X_{SCS} axes	0.285
U7	Resolution of the C_{MCS} axis	0.005
UC	Combined standard uncertainty	0.467
U	Expanded uncertainty (97% confidence level)	0.904